RESEARCH ARTICLE

DOI: 10.34256/ijcci2613

International Journal of Computer Communication and Informatics

A Wearable Multisensor Platform for Neurofibromatosis Surveillance Using Bioimpedance, Bioelectrical Signals, and TinyML

M. Vadivelan [a], R. Bhuvaneswari [a], J. Padmaja [a], N. Sajini Navab [a]

[a] Department of Biomedical Engineering, Sri Manakula Vinayagar Engineering College, Puducherry, India

* Corresponding Author: mvadivelsmve@gmail.com

Received: 17-01-2026, Revised: 20-03-2026, Accepted: 09-04-2026, Published: 21-04-2026

Abstract: Neurofibromatosis comprises genetically distinct tumour-predisposition disorders that require lifelong, risk-adapted clinical surveillance. Current follow-up relies principally on clinical examination and imaging, which are essential but intermittent and may not capture short-term changes in peripheral-nerve function or local tissue electrical properties. This paper presents the design and bench-level evaluation of a wearable, non-invasive proof-of-concept platform that combines multifrequency bioimpedance sensing, amplified peripheral bioelectrical-signal acquisition, embedded feature extraction, and TinyML-based risk-pattern classification. An AD5933 impedance-converter circuit is used to estimate impedance magnitude and phase, whereas an AD620 instrumentation-amplifier stage conditions low-amplitude nerve- or electromyography-like signals. An ESP32 microcontroller performs data acquisition, filtering, feature computation, model inference, and Bluetooth Low Energy transmission. The proposed feature set includes mean impedance, phase angle, root-mean-square amplitude, and zero-crossing rate. Bench testing with simulated impedance loads and generated bioelectrical waveforms demonstrated stable acquisition and real-time wireless display. However, the reported thresholds and classification outputs are engineering labels for prototype verification and are not validated diagnostic criteria. Patient recruitment, clinical reference standards, sensitivity, specificity, calibration, and longitudinal outcome analysis remain necessary before any clinical interpretation. The present work therefore establishes an embedded-systems architecture and feasibility workflow rather than a clinically validated neurofibromatosis diagnostic device.

Keywords: Bioimpedance Spectroscopy, Embedded Artificial Intelligence, ESP32, Neurofibromatosis, Peripheral-Nerve Monitoring, Tinyml, Wearable Biomedical System.

1. Introduction

Neurofibromatosis represents a group of inherited tumour-predisposition disorders involving the skin, peripheral nerves, central nervous system, and other organ systems. Neurofibromatosis type 1 (NF1) is characterised by age-dependent manifestations that may include café-au-lait macules, cutaneous and plexiform neurofibromas, skeletal abnormalities, learning difficulties, optic-pathway glioma, and an increased risk of malignant peripheral nerve-sheath tumour [1-3]. The former term neurofibromatosis type 2 has been replaced by NF2-related schwannomatosis under revised international nomenclature, reflecting advances in molecular classification and the clinical overlap among schwannomatosis subtypes [4, 5]. These conditions differ substantially in genetic basis, tumour spectrum, symptom burden, and surveillance requirements; consequently, a single sensor output cannot establish or exclude disease progression.

Clinical surveillance remains the standard of care. Current guidance emphasises periodic multidisciplinary assessment, symptom-triggered imaging, tumour-specific magnetic resonance imaging, hearing and ophthalmological evaluation when indicated, and age-appropriate cancer surveillance [2, 3, 6]. Whole-body MRI and computational segmentation can support tumour-burden assessment, but imaging is resource intensive and is not intended for uninterrupted ambulatory monitoring [7]. In parallel, wearable sensing and embedded intelligence have advanced sufficiently to permit low-power acquisition and local analysis of physiological signals [8]. These technologies may complement—rather than replace—clinical review by identifying signal changes that warrant further assessment.

Electrical bioimpedance measures the frequency-dependent opposition of biological tissue to an applied alternating current. Changes in hydration, cell-membrane properties, tissue composition, electrode contact, and geometry influence measured resistance and reactance. Accordingly, bioimpedance is sensitive but not disease specific. Peripheral bioelectrical signals, including surface electromyography and evoked or spontaneous nerve-related activity, provide complementary functional information but are also affected by electrode placement, motion, muscle recruitment, and environmental interference. A multimodal architecture may therefore be useful for engineering surveillance studies, provided that signal-quality control, calibration, and clinical validation are explicitly addressed [9-11].

This study proposes a wearable proof-of-concept platform that integrates AD5933-based bioimpedance acquisition, AD620-based low-amplitude signal conditioning, ESP32 processing, TinyML inference, and wireless visualisation. The objectives are to describe the hardware and software architecture, define a reproducible feature-processing pipeline, and demonstrate bench-level signal acquisition and communication. The work does not claim that the prototype detects neurofibroma growth or provides clinically validated risk stratification. Instead, it establishes the technical basis for subsequent ethics-approved studies using patient data and appropriate clinical reference standards.

2. Related Work

NF surveillance research has concentrated on clinical examination, genotype-informed follow-up, and imaging of tumour burden. Updated consensus criteria and European surveillance guidelines stress that assessment must be tailored to the patient's molecular diagnosis, age, symptoms, and tumour phenotype [2-6]. Deep interactive segmentation has also been investigated for whole-body MRI of NF1-associated neurofibromas, demonstrating the role of artificial intelligence in image-assisted tumour quantification [7]. These approaches address clinically established imaging workflows but do not provide continuous peripheral physiological sensing.

Bioimpedance spectroscopy has been applied to body-composition estimation, hydration assessment, tissue characterisation, electrode-contact monitoring, and several exploratory diagnostic applications. Its principal advantages are low excitation energy, portability, and compatibility with embedded hardware. Its limitations include dependence on calibration, electrode–skin interface quality, excitation frequency, anatomical geometry, temperature, and motion [9, 10]. The AD5933 provides a compact frequency generator and impedance-measurement engine, but biomedical implementation requires an appropriate analogue front end, current limitation, calibration impedance, and patient-safety isolation [12].

Wearable electrophysiological systems similarly require high common-mode rejection, low-noise amplification, protection circuitry, and robust artefact suppression. The AD620 instrumentation amplifier is suitable for prototype amplification of low-level differential signals, although the complete acquisition chain must still meet medical-electrical safety and electromagnetic-compatibility requirements [13]. TinyML frameworks enable compressed machine-learning models to run on microcontrollers with limited memory and power budgets. On-device inference can reduce communication latency and data exposure, but model validity depends on representative training data, transparent preprocessing, external validation, and careful control of dataset leakage [14, 15].

The present work combines these engineering elements in one prototype. The specific contribution is architectural integration and bench demonstration. The unresolved research gap is clinical validation: there is currently insufficient evidence to treat bioimpedance and surface nerve-signal features as established biomarkers of neurofibromatosis progression.

3. Methodology

3.1 System Architecture

Figure 1 presents the end-to-end architecture. Surface electrodes provide two acquisition pathways. The first pathway uses the AD5933 to generate a controlled sinusoidal excitation and estimate complex impedance. The second pathway uses an AD620 instrumentation-amplifier stage to condition low-amplitude peripheral bioelectrical signals. The ESP32 coordinates

sampling, preprocessing, feature extraction, TinyML inference, and Bluetooth Low Energy communication. A mobile or computer dashboard displays the processed values and prototype class output. The power subsystem supplies regulated rails to the analogue and digital blocks.

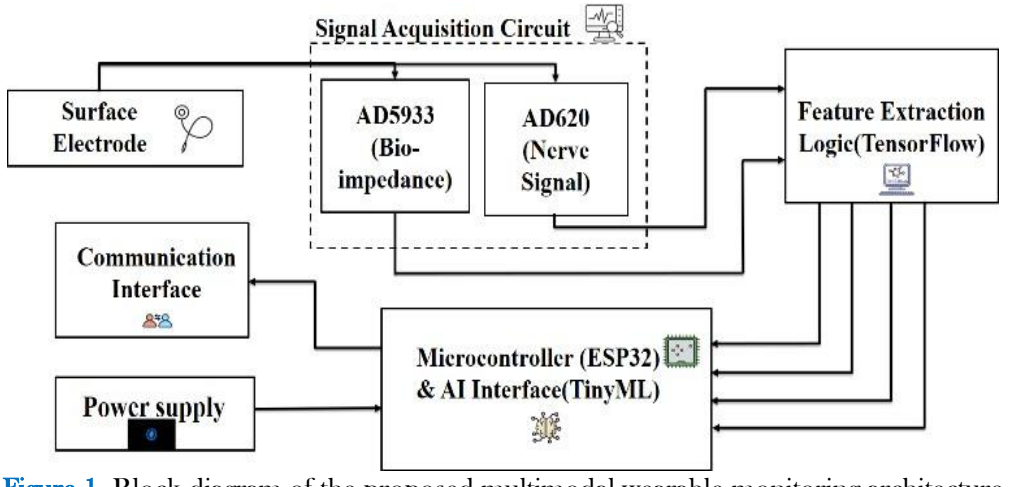

Figure 1. Block diagram of the proposed multimodal wearable monitoring architecture

3.2 Hardware Components

The sensing interface uses disposable or reusable surface electrodes selected according to the intended measurement mode. Bioimpedance measurements require a defined electrode configuration, controlled excitation amplitude, and calibration with a known reference impedance. The AD5933 communicates with the ESP32 through the I²C bus. Because the AD5933 alone is not a complete human-connected bioimpedance instrument, the prototype design must include current limiting, analogue buffering, protection, and electrical isolation before any volunteer study [12].

The AD620 stage provides differential amplification for the peripheral bioelectrical channel. Gain is set by an external resistor, and analogue high-pass, low-pass, and mains-frequency rejection stages are used as required by the selected signal bandwidth. The amplified output is constrained to the ESP32 analogue-to-digital converter input range. Electrode placement, skin preparation, cable motion, and reference-electrode stability are controlled because these variables can dominate the recorded waveform [13].

The ESP32 was selected because it integrates a microcontroller, analogue-to-digital conversion, I²C communication, and Bluetooth connectivity in a compact platform [16]. It executes deterministic acquisition tasks and a small inference model. This prototype is intended for laboratory evaluation; a future human-use version would require compliance with applicable medical-device risk-management, electrical-safety, biocompatibility, cybersecurity, and software-life-cycle standards.

3.3 Signal Acquisition and Preprocessing

For the impedance channel, the device performs a frequency sweep over a predefined band and records the real and imaginary response components after calibration. Repeated measurements are averaged to reduce random variation. For the peripheral bioelectrical channel, the ESP32 samples the conditioned waveform at a fixed rate. Baseline removal, band-limited digital filtering, and amplitude clipping checks are applied before feature extraction. Windows contaminated by saturation, electrode detachment, or excessive motion should be rejected rather than classified.

Bench evaluation used known resistor–capacitor loads to emulate different complex impedances and generated low-amplitude waveforms to exercise the electrophysiological channel. No patient-derived dataset was reported in the source manuscript. Therefore, all results in this paper are interpreted as engineering verification only.

3.4 Feature Extraction

Complex impedance is represented by

$$Z = R + jX \tag{1}$$

Where R is resistance and X is reactance. Impedance magnitude and phase are calculated as

$$|Z| = \sqrt{(R^2 + X^2)} \tag{2}$$

$$\varphi = tan^{-1}(X/R) \tag{3}$$

For a sampled peripheral bioelectrical window x(n) containing N samples, the root-mean-square amplitude is

$$RMS = \sqrt{[(1/N)\,\Sigma\, x(n)^2]},\ n = 1, \ldots, N \tag{4}$$

The zero-crossing rate is computed as the number of sign changes per unit time after applying a small dead band to suppress noise-induced crossings. When spectral features are required, the discrete Fourier transform is

$$X(k) = \Sigma\, x(n)e\text{^}(-j2\pi kn/N),\ k = 0, \ldots, N-1 \tag{5}$$

Only features defined before model training should be retained. Scaling parameters must be estimated from the training partition and then applied unchanged to validation and test data to prevent information leakage.

3.5 TinyML Model and Prototype Labels

A compact feed-forward neural network can accept four inputs: mean impedance, mean phase, RMS amplitude, and zero-crossing rate. One or two small dense layers with rectified-linear activation are followed by a three-node softmax output. Training is performed offline, after which the quantised TensorFlow Lite model is deployed on the ESP32 using a microcontroller inference runtime [14, 15].

Table 1 lists the engineering thresholds supplied in the prototype dataset. They are retained solely to reproduce the software demonstration. They are not derived from a clinical cohort, do not correspond to accepted NF diagnostic criteria, and must not be used for patient management. A clinical study would require prospectively defined outcomes, expert-labelled reference data, prespecified inclusion criteria, independent testing, and reporting of discrimination, calibration, uncertainty, and subgroup performance.

Table 1. Prototype Feature Thresholds Used For Software Verification

Parameter (unit)	No-risk label	Low-risk label	High-risk label
Mean impedance (Ω)	190–230	>230–330	>330
Mean phase (°)	>−20	−20 to −35	≤−35
Nerve RMS (V)	<0.04	0.04–0.07	>0.07
Nerve ZCR (Hz)	0.05–0.12	>0.12–0.20	>0.20

3.6 Software Implementation

The firmware initialises the AD5933, analogue-to-digital converter, filters, Bluetooth interface, and inference model. Each acquisition cycle collects impedance and waveform data, performs quality checks, computes the selected features, applies stored normalisation parameters, executes inference, and transmits a compact packet containing the feature values, signal-quality flags, and prototype class. The dashboard plots trends and displays warnings when the input is outside the calibrated range. Raw-data retention, encryption, user authentication, and audit logging should be implemented before clinical deployment.

4. Results and Discussion

Bench testing showed that the AD5933 pathway produced repeatable values for the resistor–capacitor loads used during prototype evaluation. The AD620 pathway also reproduced the generated low-amplitude waveforms sufficiently to calculate RMS and zero-crossing features. Bluetooth transmission supported continuous dashboard updating during the reported test interval. Figure 2 shows representative software output from successive acquisition windows.

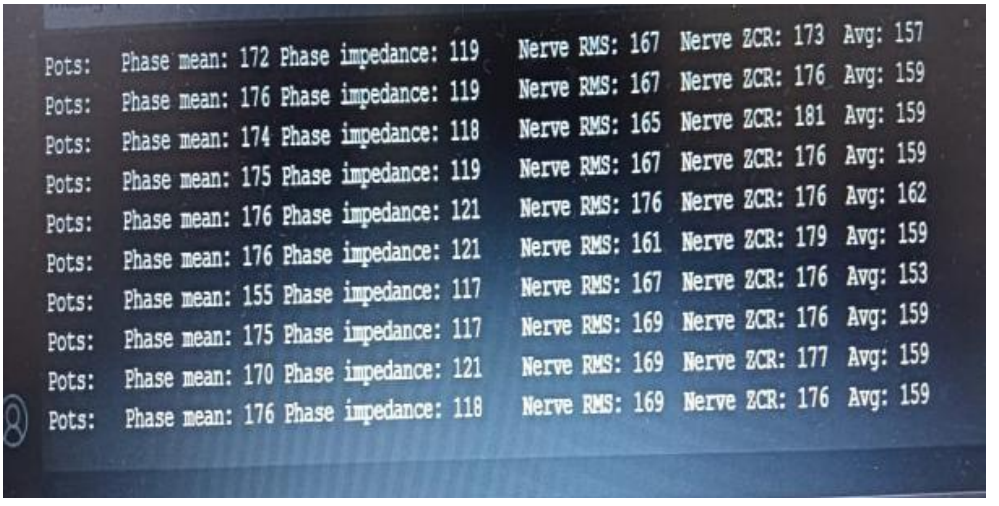

Figure 2. Representative software output showing successive feature values during bench-level prototype testing

The screenshot confirms data flow through the acquisition, feature-extraction, display, and communication pipeline. It does not establish measurement accuracy because the source manuscript does not report reference-instrument comparisons, error distributions, confidence intervals, sampling duration, number of repeated trials, or environmental test conditions. Likewise, the TinyML output demonstrates executable inference but not clinical classification performance. No confusion matrix, receiver-operating-characteristic analysis, sensitivity, specificity, calibration plot, or independent test cohort was available.

The main technical strength is multimodal integration on a low-cost embedded platform. The main limitations are more consequential: absence of patient-derived data; absence of ethics and consent information; unvalidated thresholds; no documented electrode geometry or excitation-current safety analysis; incomplete analogue-filter specifications; no power-consumption or battery-life measurements; and no comparison with clinical or laboratory reference systems. Bioimpedance is also highly sensitive to contact and geometry, whereas surface bioelectrical activity is influenced by muscle activation and motion. Consequently, observed changes cannot presently be attributed specifically to neurofibroma growth or nerve dysfunction.

A rigorous next-stage study should proceed in two steps. First, laboratory validation should quantify impedance error across known loads, frequency-dependent repeatability, electrophysiological gain and noise, artefact rejection, wireless packet loss, latency, and energy consumption. Second, an ethics-approved observational study should compare longitudinal wearable features with predefined clinical assessments and imaging outcomes. Model development should use patient-level data partitioning, nested validation where appropriate, and external testing at a separate site.

5. Conclusion

This study presents a wearable embedded-AI architecture that combines bioimpedance sensing, low-amplitude peripheral bioelectrical-signal acquisition, ESP32-based feature extraction, TinyML inference, and Bluetooth visualisation for exploratory neurofibromatosis surveillance. The prototype demonstrates end-to-end acquisition and real-time software operation under bench conditions. The revised interpretation is deliberately limited: the system is not a validated diagnostic or monitoring device, and the supplied thresholds are software-verification labels rather than clinically established decision limits. Publication of the architecture is nevertheless useful because it identifies a compact implementation pathway and the validation requirements that must be satisfied before human use. Future work should prioritise electrical-safety engineering, traceable calibration, complete reporting of hardware and firmware parameters, controlled laboratory benchmarking, ethics-approved patient studies, independent model validation, and comparison with accepted clinical reference standards. Only after these steps can the value of multimodal wearable sensing for longitudinal neurofibromatosis management be determined.

6. Future Work

Future development should include a medically appropriate isolated analogue front end, four-electrode bioimpedance measurement where feasible, electrode-contact quality estimation, adaptive motion-artifact rejection, and power profiling under realistic duty cycles. The software should preserve raw and processed data with time stamps, calibration metadata, signal-quality flags, and secure transmission. Clinical evaluation should recruit a sufficiently diverse cohort, define the target condition and outcome precisely, and compare device outputs against specialist examination, imaging, and electrophysiological reference tests. The final model should report uncertainty and abstain when signal quality is inadequate or the input lies outside the validated operating domain.

References

[1] E. Legius, L. Messiaen, P. Wolkenstein, P. Pancza, R.A. Avery, Y.Berman, J. Blakeley,• D.B. Vuksanovic, K.S. Cunha, R. Ferner, M.J. Fisher, J.M. Friedman, D.H. Gutmann, H. Kehrer-Sawatzki, B.R. Korf, V.F. Mautner, S. Peltonen, K.A. Rauen, V. Riccardi, E. Schorry, A. Stemmer-Rachamimov, D.A. Stevenson, G. Tadini, N.J. Ullrich, D. Viskochil, K. Wimmer, K. Yohay A. Gomes, J. T. Jordan, V. Mautner, V. L. Merker, M. J. Smith, D. Stevenson, M. Anten, A. Aylsworth, D. Baralle, S. Barbarot, F. Barker, S. Ben-Shachar, A. Bergner, D. Bessis, I. Blanco, C. Cassiman, P. Ciavarelli, M. Clementi, T. Frébourg, M. Giovannini, D. Halliday, C. Hammond, C.O. Hanemann, H. Hanson, A. Heiberg, P. Joly, M. Kalamarides, M. Karajannis, D. Kroshinsky, M. Larralde, C.

Lázaro, L. Le, M. Link, R. Listernick, M. MacCollin, C. Mallucci, C. Moertel , A. Mueller, J. Ngeow, R. Oostenbrink, R. Packer, L. Papi, A. Parry, J. Peltonen, D. Pichard, B. Poppe, N. Rezende, L.O. Rodrigues, T. Rosser, M. Ruggieri, E. Serra, V. Steinke-Lange, S.M. Stivaros, A. Taylor, J. Toelen, J. Tonsgard, E. Trevisson, M. Upadhyaya, A. Varan, M. Wilson, H. Wu, G. Zadeh, S.M. Huson, D.G. Evans, S.R. Plotkin, Revised diagnostic criteria for neurofibromatosis type 1 and Legius syndrome: an international consensus recommendation. Genetics in medicine, 23(8), (2021) 1506-1513. https://doi.org/10.1038/s41436-021-01170-5

[2] C. Carton, D. Gareth Evans, I. Blanco, R.E. Friedrich, R.E. Ferner, S. Farschtschi, H. Salvador, A.A. Azizi, V. Mautner, C. Röhl, S. Peltonen, S. Stivaros, E. Legius, R. Oostenbrink, ERN GENTURIS tumour surveillance guidelines for individuals with neurofibromatosis type 1. eClinicalMedicine, 56, (2023) 101818. https://doi.org/10.1016/j.eclinm.2022.101818

[3] D.R. Stewart, B.R. Korf, K.L. Nathanson, D.A. Stevenson, K. Yohay, Care of adults with neurofibromatosis type 1: a clinical practice resource of the American College of Medical Genetics and Genomics (ACMG). Genetics in Medicine, 20(7), (2018) 671-682. https://doi.org/10.1038/gim.2018.28

[4] [4] S.R. Plotkin, Ludwine Messiaen, Eric Legius, Patrice Pancza, Robert A. Avery, Jaishri O. Blakeley, · Dusica Babovic-Vuksanovic, Rosalie Ferner, Michael J. Fisher, Jan M. Friedman, ,Marco Giovannini,· David H. Gutmann, Clemens Oliver Hanemann, Michel Kalamarides, Hildegard Kehrer-Sawatzki, · Bruce R. Korf, Victor-Felix Mautner, Mia MacCollin, Laura Papi, Katherine A. Rauen, Vincent Riccardi, Elizabeth Schorry, Miriam J. Smith, Anat Stemmer-Rachamimov, David A. Stevenson, Nicole J. Ullrich, David Viskochil, Katharina Wimmer, Kaleb Yohay, International Consensus Group on Neurofibromatosis Diagnostic Criteria (I-NF-DC) · S.M. Huson, Pierre Wolkenstein, D. Gareth Evans, Updated diagnostic criteria and nomenclature for neurofibromatosis type 2 and schwannomatosis: An international consensus recommendation. Genetics Medicine, 24(9), (2022) 1967–1977. https://doi.org/10.1016/j.gim.2022.05.007

[5] D.G. Evans, S. Mostaccioli, D. Pang, Fadzil M. O Connor, M. Pittara, N. Champollion, P. Wolkenstein, N. Thomas, R.E. Ferner, M. Kalamarides, M. Peyre, L. Papi, E. Legius, J. Luis Becerra, A. King, C. Duff, S. Stivaros, I. Blanco, Ern Genturis clinical practice guidelines for the diagnosis, treatment, management and surveillance of people with schwannomatosis. European Journal of Human Genetics, 30(7), (2022) 812-817. https://doi.org/10.1038/s41431-022-01086-x

[6] M.R. Perrino, A.Das, S.R. Scollon, S.G. Mitchell, M.L.C. Greer, M.E. Yohe, J.R. Hansford, J.M. Kalish, K.A.P. Schultz, S.P. MacFarland, W.K. Kohlmann, P.J. Lupo, K.N. Maxwell, S.M. Pfister, R. Weksberg, O. Michaeli, M.C.J. Jongmans, G.E. Tomlinson, J. Brzezinski, U. Tabori, G.M. Ney, K.W. Gripp, A.M. Gross, B.C. Widemann, D.R. Stewart, E.R. Woodward, C.P. Kratz, Update on pediatric cancer surveillance recommendations for patients with neurofibromatosis type 1 and related

RASopathies. Clinical Cancer Research, 30(21), (2024) 4834–4843. https://doi.org/10.1158/1078-0432.CCR-24-1611

[7] J.W. Zhang, W. Chen, K.I. Ly, X. Zhang, F. Yan, J. Jordan, G. Harris, S. Plotkin, P. Hao, W. Cai, DINs: Deep interactive networks for neurofibroma segmentation in neurofibromatosis type 1 on whole-body MRI. IEEE journal of biomedical and health informatics, 26(2), (2021) 786-797.

[8] J. Kim, A.S. Campbell, B.EF. de Ávila, J. Wang, Wearable biosensors for healthcare monitoring. Nat Biotechnol 37, 389–406 (2019). https://doi.org/10.1038/s41587-019-0045-y

[9] S. Grimnes, Ø.G. Martinsen, (2014). Bioimpedance and bioelectricity basics. Academic press.

[10] U.G. Kyle, I. Bosaeus, A.D. De Lorenzo, P. Deurenberg, M. Elia, J.M. Gómez, B.L. Heitmann, L. Kent-Smith, J.C. Melchior, H. Scharfetter, A.M.W.J. Schols, Claude Pichardm, Composition of the ESPEN Working Group, C. Pichard, Bioelectrical impedance analysis—part I: review of principles and methods. Clinical nutrition, 23(5), (2004) 1226-1243. https://doi.org/10.1016/j.clnu.2004.06.004

[11] R. Merletti, D. Farina, (2016) Surface Electromyography: Physiology, Engineering, and Applications. Hoboken, Wiley-IEEE Press.

[12] Analog Devices, (2017) AD5933: 1 MSPS, 12-bit impedance converter, network analyzer. Data Sheet, Rev. F. Analog Devices.

[13] Analog Devices, (2011) AD620: Low cost, low power instrumentation amplifier. Data Sheet, Rev. K. Analog Devices.

[14] R. David, J. Duke, A. Jain, V. Janapa Reddi, N. Jeffries, J. Li, N. Kreeger, I. Nappier, M. Natraj, S. Regev, R. Rhodes, T. Wang, P. Warden, TensorFlow Lite Micro: Embedded machine learning for TinyML systems. arXiv: 2010.08678v2.

[15] P. Warden, D. Situnayake, (2019) TinyML: Machine Learning with TensorFlow Lite on Arduino and Ultra-Low-Power Microcontrollers. O'Reilly Media, Sebastopol, CA, USA.

[16] Datasheet, S. (2021). ESP32 Series Datasheet. Espressif System Datasheet, 1-31.

Funding

No funding was received for conducting this study.

Conflict of interest

The Author have no conflicts of interest to declare that they are relevant to the content of this article.

About The License